Explaining Latent Representations with a Corpus of Examples

Anonymous Author(s)
Affiliation
Address
email

Abstract

Modern machine learning models are complicated. Most of them rely on convoluted latent representations of their input to issue a prediction. To achieve greater transparency than a black-box that connects inputs to predictions, it is necessary to gain a deeper understanding of these latent representations. To that aim, we propose SimplEx: a user-centred method that provides example-based explanations with reference to a freely selected set of examples, called the corpus. SimplEx uses the corpus to improve the user's understanding of the latent space with post-hoc explanations answering two questions: (1) Which corpus examples explain the prediction issued for a given test example? (2) What features of these corpus examples are relevant for the model to relate them to the test example? SimplEx provides an answer by reconstructing the test latent representation as a mixture of corpus latent representations. Further, we propose a novel approach, the integrated Jacobian, that allows SimplEx to make explicit the contribution of each corpus feature in the mixture. Through experiments on tasks ranging from mortality prediction to image classification, we demonstrate that these decompositions are robust and accurate. With illustrative use cases in medicine, we show that SimplEx empowers the user by highlighting relevant patterns in the corpus that explain model representations. Moreover, we demonstrate how the freedom in choosing the corpus allows the user to have personalized explanations in terms of examples that are meaningful for them.

1 Introduction and related work

How can we make a machine learning model convincing? If accuracy is undoubtedly necessary, it is rarely sufficient. As these models are used in critical areas such as medicine, finance and the criminal justice system, their black-box nature appears as a major issue [1, 2, 3]. With the necessity to address this problem, the landscape of explainable artificial intelligence (XAI) developed [4, 5]. This landscape is rich, in this work we will center our discussion around post-hoc explainability techniques. These techniques aim at improving the interpretability of models that are not interpretable by design by complementing the predictions of these models with various kind of explanations.

The most popular family of post-hoc explanations found in the XAI litterature is undoubtedly the family of feature saliency methods. These methods complement the model prediction for an input example with a score attributed at each input feature. This score reflects the importance of each feature for the model to issue its prediction. Popular examples of such methods include SHAP [6, 7, 8], LIME [9], Integrated Gradient [10] and Contrastive Examples [11]. Knowing which feature are important for a model prediction certainly provides more information on the model than the prediction by itself. However, these methods do not provide a reason as to why the model pays attention to these

Submitted to 35th Conference on Neural Information Processing Systems (NeurIPS 2021). Do not distribute.

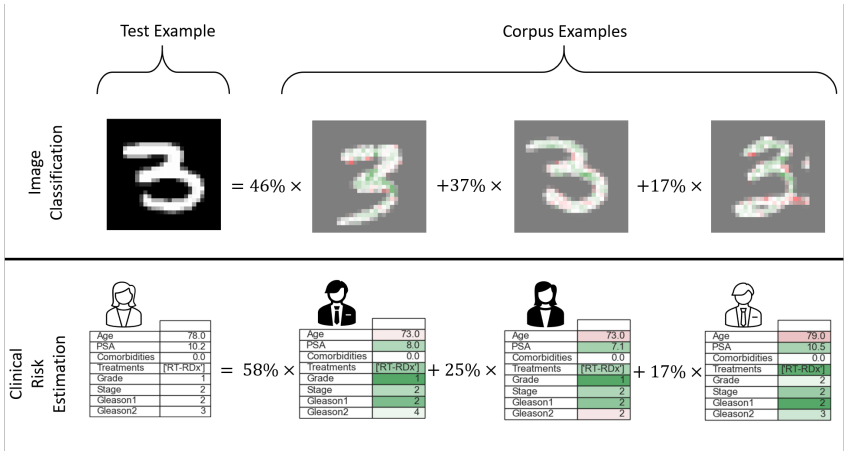

Figure 1: An example of corpus decomposition with SimplEx.

particular features. If we want to explore these reasons, it is necessary to take a step back and think about the model's origin.

Every model is obtained by finding patterns in data that are useful for the model's purpose. If a model pays attention to particular features, it is because these features help to detect patterns. Hence, a way to go beyond a feature saliency explanation is to contextualize this saliency as emerging from a pattern. This motivates an example-based approach of explainability, where each prediction is contextualized with the help of relevant data. This approach is commonly known as *Case-Based Reasoning* (CBR) [12, 13, 14]. The implementations of CBR generally involve models that create a synthetic representation of the dataset, where examples with similar paterns are summarized by prototypes [15, 16, 17]. At inference time, these models relate new examples to one or several prototypes to issue a prediction. In this way, the patterns that are used by the model to issue a prediction are made explicit with the help of relevant prototypes. A limitation of this approach is the restricted model architecture. The aforementioned procedure requires to opt for a family of models that rely on prototypes to issue a prediction. This family of model might not always be the most suitable for the task at hand. This motivates the development of generic post-hoc methods that work by making few or no assumption on the model.

The most common approach to provide example-based explanations for a wide variety of models mirrors feature saliency methods. The idea is to complement the model prediction with a score attributed at each training example. This score reflects the importance of each training example for the model to issue its prediction. This will typically be done by simulating the effect of removing each training instance from the training set on the learned model [18]. Popular examples of such methods include Influence Functions [19] and Data-Shapley [20, 21]. These methods offer the advantage of being flexible enough to be used with a wide variety of models. They produce scores that describe what the model could have predicted if some examples were absent from the training set. This is very interesting in a data valuation perspective. However, unlike CBR methods, it does not explain the model predictions with reference to the underlying training examples.

So far, we have only discussed works that provide explanations of a model output, which is the tip of the iceberg. Modern machine learning models involve many convoluted transformations to deduce the output from an input. These transformations are expressed in terms of intermediate variables that are often called *latent variables*. Some treatment of these latent variables is necessary if we want to provide explanations that take the model complexity into account. This motivates several works that push the explainability task beyond the realm of model outputs. Among the most noticeable contributions in this endeavour, we cite *Concept Activation Vectors* that create a dictionary between human friendly concepts (such as the presence of stripes in an image) and their representation in terms of latent vectors [22]. Another interesting contribution is the *Deep k-Nearest Neighbors* models that contextualize the prediction for an example with its Nearest Neighbours in the space of latent variables, the *latent space* [23]. Another interesting exploration of the latent space is offered by the *representer theorem* that allows, under restrictive assumptions, to use latent vectors to decompose a model's prediction in terms of its training examples [24].

Contribution In this work, we introduce a novel approach called SimplEx that lies at the crossroad of the above research directions. SimplEx outputs post-hoc explanations in the form of Figure 1, where the model's prediction and latent representation for a test example is approximated as a mixture of examples extracted from a *corpus* of examples. In each case, SimplEx highlights the role played by each feature of each corpus example in the latent space decomposition. The meaning of the colour attributed to each feature is explained in Section 2. SimplEx centralizes many functionalities that, to the best of our knowledge, constitute a leap forward from the previous state of the art. (1) SimplEx gives the user freedom to choose the corpus of examples whom with the model's predictions are decomposed. Unlike previous methods such as the representer theorem, there is no need for this corpus of example to be equal to the model's training set. This is particularly interesting for two reasons: (a) the training set of a model is not always accesible (b) the user might want exaplanations in terms of examples that make sense for them. For instance, a doctor might want to understand the predictions of a risk model in terms of patients they knows. (2) The decompositions of SimplEx are valid, both in latent and output space. We show that, in both cases, the corpus mixtures discovered by SimplEx offer significantly more precision and robustness than previous methods such as Deep k-Nearest Neighbors and the representer theorem. (3) SimplEx details the role played by each feature in the corpus mixture. This is done by introducing Integrated Jacobian, a generalization of Integrated Gradient, that makes the contribution of each corpus feature explicit in the latent space decomposition. This creates a bridge between two research directions that have mostly developped independently: feature saliency and example-based explanations [14, 25].

2 Mathematical formulation

In this section, we formulate our method rigorously. Our purpose is to explain the black-box prediction for an unseen test example with the help of a set of known examples that we call the *corpus*. We start with a clear statement of the family of black-boxes for which our method applies. Then, we detail how the set of corpus examples can be used to decompose a black-box representation for the unseen example. Finally, we show that the corpus decomposition can offer explanations at the feature level.

2.1 Preliminaries

Let $\mathcal{X} \subseteq \mathbb{R}^{d_X}$ be an input (or feature) space and $\mathcal{Y} \subseteq \mathbb{R}^{d_Y}$ be an output (or label) space, where d_X and d_Y are respectively the dimension of the input and the output space. Our task is to explain individual predictions of a given black-box $\mathbf{f} : \mathcal{X} \to \mathcal{Y}$. In order to build our explainability method, we need to make an assumption on the family of black-boxes that we wish to interpret.

Assumption 2.1 (Black-box Restriction)**.** We restrict to black-boxes $\mathbf{f} : \mathcal{X} \to \mathcal{Y}$ that can be decomposed as $\mathbf{f} = \mathbf{l} \circ \mathbf{g}$, where $\mathbf{g} : \mathcal{X} \to \mathcal{H}$ maps an input $\mathbf{x} \in \mathcal{X}$ to a latent vector $\mathbf{h} = \mathbf{g}(\mathbf{x}) \in \mathcal{H}$ and $\mathbf{l} : \mathcal{H} \to \mathcal{Y}$ linearly maps[1] a latent vector $\mathbf{h} \in \mathcal{H}$ to an output $\mathbf{y} = \mathbf{l}(\mathbf{h}) = \mathbf{A}\mathbf{h} \in \mathcal{Y}$. In the following, we call $\mathcal{H} \subseteq \mathbb{R}^{d_H}$ the *latent space*. Typically, this space has higher dimension than the output space $d_H > d_Y$.

Remark 2.1. In the context of deep-learning, this assumption requires that the last hidden layer maps linearly to the output. While it is often the case, it is crucial in the following since we will use the fact that linear combinations in latent space correspond to linear combinations in output space. Our purpose is to gain insights on the structure of the latent space.

Remark 2.2. This assumption is compatible with regression and classification models, we just need to clarify what we mean by *output* in the case of classification. If $\mathbf{f}$ is a classification black-box that predicts the probabilities for each class, it will typically take the form in Assumption 2.1 up to a normalizing map $\boldsymbol{\phi}$ (typically a softmax): $\mathbf{f} = \boldsymbol{\phi} \circ \mathbf{l} \circ \mathbf{g}$. In this case, we ignore[2] the normalizing map $\boldsymbol{\phi}$ and define the output to be $\mathbf{y} = (\mathbf{l} \circ \mathbf{g})(\mathbf{x})$.

Our explanations for $\mathbf{f}$ rely on a set of examples that we call the corpus. These examples will typically (but not necessarily) be a representative subset of the black-box training set. The corpus set has to be understood as a set of reference examples that we want to use as building blocks to interpret unseen examples. In order to index these examples, it will be useful to denote by $[n_1 : n_2]$ the set of natural numbers between the natural numbers n_1 and n_2 with $n_1 < n_2$. Further, we denote $[n] = [1 : n]$ the

[1] The map can in fact be affine. In the following, we omit the bias term $\mathbf{b} \in \mathcal{Y}$ that can be reabsorbed in $\mathbf{g}$.

[2] There is no loss or information as the output allows us to reconstruct class probabilities $\mathbf{p}$ via $\mathbf{p} = \boldsymbol{\phi}(\mathbf{y})$.

set of natural numbers between 1 and $n \geq 1$. The corpus of examples is a set $\mathcal{C} = \{\mathbf{x}^c \mid c \in [C]\}$ containing $C \in \mathbb{N}^*$ examples $\mathbf{x}^c \in \mathcal{X}$. In the following, superscripts are labels for examples and subscripts are labels for vector components. In this way, x_i^c has to be understood as the component i of corpus example c.

2.2 A corpus of examples to explain a latent representation

Our purpose is to understand a prediction $\mathbf{f}(\mathbf{x})$ for an unseen test example $\mathbf{x}$ with the help of the corpus. How can we decompose the prediction $\mathbf{f}(\mathbf{x})$ in terms of corpus predictions $\mathbf{f}(\mathbf{x}^c)$? A naive attempt would be to express $\mathbf{x}$ as a mixture of inputs from the corpus $\mathcal{C}$: $\mathbf{x} = \sum_{c=1}^{C} w^c \mathbf{x}^c$ with weights $w^c \in [0,1]$ that sum to one $\sum_{c=1}^{C} w^c = 1$. The weakness of this approach is that the signification of the mixture weights is not conserved if the black-box $\mathbf{f}$ is not a linear map: $\mathbf{f}(\sum_{c=1}^{C} w^c \mathbf{x}^c) \neq \sum_{c=1}^{C} w^c \mathbf{f}(\mathbf{x}^c)$.

Fortunately, Assumption 2.1 offers us a better vector space to perform a corpus decomposition of the unseen example $\mathbf{x}$. We first note that the map $\mathbf{g}$ induces a latent representation of the corpus $\mathbf{g}(\mathcal{C}) = \{\mathbf{h}^c = \mathbf{g}(\mathbf{x}^c) \mid \mathbf{x}^c \in \mathcal{C}\} \subset \mathcal{H}$. Similarly, $\mathbf{x}$ has a latent representation $\mathbf{h} = \mathbf{g}(\mathbf{x}) \in \mathcal{H}$. Following the above line of reasoning, we could therefore perform a corpus decomposition in latent space $\mathbf{h} = \sum_{c=1}^{C} w^c \mathbf{h}^c$. Now, by using the linearity of $\mathbf{l}$, we can compute the black-box output of this mixture in latent space: $\mathbf{l}(\sum_{c=1}^{C} w^c \mathbf{h}^c) = \sum_{c=1}^{C} w^c \mathbf{l}(\mathbf{h}^c)$. In this case, the weights that are used to decompose the latent representation $\mathbf{h}$ in terms of the latent representation of the corpus $\mathbf{g}(\mathcal{C})$ also reflect the way in which the black-box prediction $\mathbf{f}(\mathbf{x})$ can be decomposed in terms of the corpus outputs $\mathbf{f}(\mathcal{C})$. This hints that the latent space $\mathcal{H}$ is endowed with the appropriate geometry to make corpus decompositions. More formally, we think in terms of the convex hull spanned by the corpus.

Definition 2.1 (Corpus Hull)**.** The *corpus convex hull* spanned by a corpus $\mathcal{C}$ with latent representation $\mathbf{g}(\mathcal{C}) = \{\mathbf{h}^c = \mathbf{g}(\mathbf{x}^c) \mid \mathbf{x}^c \in \mathcal{C}\} \subset \mathcal{H}$ is the convex set

$$\mathcal{CH}(\mathcal{C}) = \left\{ \sum_{c=1}^{C} w^c \mathbf{h}^c \;\middle|\; w^c \in [0,1]\ \forall c \in [C] \ \wedge \ \sum_{c=1}^{C} w^c = 1 \right\}.$$

Remark 2.3. This is the set of latent vectors that are a mixture of the corpus latent vectors.

At this stage, it is important to notice that an exact corpus decomposition is not possible if $\mathbf{h} \notin \mathcal{CH}(\mathcal{C})$. In such a case, the best we can do is to find the element $\hat{\mathbf{h}} \in \mathcal{CH}(\mathcal{C})$ that best approximates $\mathbf{h}$. If $\mathcal{H}$ is endowed with a norm[3] $\| \cdot \|_{\mathcal{H}}$, this corresponds to the convex optimization problem

$$\hat{\mathbf{h}} = \underset{\tilde{\mathbf{h}} \in \mathcal{CH}(\mathcal{C})}{\arg\min} \ \| \mathbf{h} - \tilde{\mathbf{h}} \|_{\mathcal{H}} \ . \tag{1}$$

By definition, the corpus representation $\hat{\mathbf{h}}$ of $\mathbf{h}$ can be expanded as a mixture of elements from $\mathbf{g}(\mathcal{C})$: $\hat{\mathbf{h}} = \sum_{c=1}^{C} w^c \mathbf{h}^c$. The weight can naturally be interpreted as a measure of saliency in the reconstruction of $\mathbf{h}$ with the corpus. Clearly, $w^c \approx 0$ for some $c \in [C]$ indicates that $\mathbf{h}^c$ does not play a significant role in the corpus representation $\hat{\mathbf{h}}$ of $\mathbf{h}$. On the other hand, $w^c \approx 1$ indicates that $\mathbf{h}^c$ generates the corpus representation $\hat{\mathbf{h}}$ by itself.

At this stage, a natural question arises: how can we know if the corpus approximation $\hat{\mathbf{h}}$ is faithful to $\mathbf{h}$? The answer is given by the residual vector $\mathbf{h} - \hat{\mathbf{h}}$ that measures the shift between the latent representation $\mathbf{h} = \mathbf{g}(\mathbf{x})$ and the corpus hull $\mathcal{CH}(\mathcal{C})$. It is natural to use this residual vector to detect examples that cannot be explained with the selected corpus of examples $\mathcal{C}$.

Definition 2.2 (Corpus Residual)**.** The *corpus residual* associated to a latent vector $\mathbf{h} \in \mathcal{H}$ and its corpus representation $\hat{\mathbf{h}} \in \mathcal{CH}(\mathcal{C})$ solving (1) is the quantity

$$r_{\mathcal{C}}(\mathbf{h}) = \| \mathbf{h} - \hat{\mathbf{h}} \|_{\mathcal{H}} = \min_{\tilde{\mathbf{h}} \in \mathcal{CH}(\mathcal{C})} \| \mathbf{h} - \tilde{\mathbf{h}} \|_{\mathcal{H}} \ .$$

[3] In our implementation, we minimize the squared 2-norm on $\mathcal{H}$.

In Section 1.1 of the supplementary material, we show that the corpus residual also controls the quality of the corpus approximation in output space $\mathcal{Y}$. All the corpus-related quantities that we have introduced so far are summarized visually in Figure 2. Note that this Figure is a simplification of the reality as the number of corpus examples C will typically be larger than 3 and the dimension of the input and latent spaces will typically be higher than 2. We are now endowed with a rigorous way to decompose a test example in terms of corpus examples *in latent space*. In the next section, we detail how to pull-back this decomposition in input space.

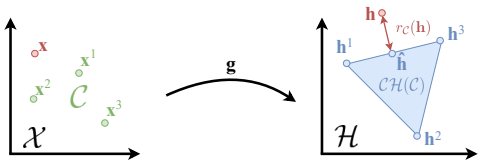

Figure 2: Corpus convex hull and residual.

2.3 Transferring the corpus explanation in input space

Now that we are endowed with a corpus decomposition $\hat{\mathbf{h}} = \sum_{c=1}^{C} w^c \mathbf{h}^c$ that approximates $\mathbf{h}$, it would be convenient to have an understanding of the corpus decomposition in input space $\mathcal{X}$. For the sake of notation, we will assume that the corpus approximation is good so that we do no longer need to draw a distinction between the latent representation $\mathbf{h}$ of the unseen example $\mathbf{x}$ and its corpus decomposition $\hat{\mathbf{h}}$. If we want to understand the corpus decomposition in input space, a natural approach is to fix a baseline input $\mathbf{x}^0$ together with its latent representation $\mathbf{h}^0 = \mathbf{g}(\mathbf{x}^0)$. Let us now decompose the representation shift $\mathbf{h} - \mathbf{h}^0$ in terms of the corpus:

$$\mathbf{h} - \mathbf{h}^0 = \sum_{c=1}^{C} w^c \left(\mathbf{h}^c - \mathbf{h}^0\right). \tag{2}$$

With this decomposition, we understand the total shift in latent space $\mathbf{h} - \mathbf{h}^0$ in terms of individual contributions from each corpus member. In the following, we focus on the comparison between the baseline and a single corpus example $\mathbf{x}^c$ together with its latent representation $\mathbf{h}^c$ by keeping in mind that the full decomposition (2) can be reconstructed with the whole corpus. To bring the discussion in input space $\mathcal{X}$, we interpret the shift in latent space $\mathbf{h}^c - \mathbf{h}^0$ as resulting from a shift $\mathbf{x}^c - \mathbf{x}^0$ in the input space. We are interested in the contribution of each feature to the latent space shift. To decompose the shift in latent space in terms of the features, we parametrize the shift in input space with a line $\boldsymbol{\gamma}^c : [0,1] \to \mathcal{X}$ that goes from the baseline to the corpus example: $\boldsymbol{\gamma}^c(t) = \mathbf{x}^0 + t \cdot (\mathbf{x}^c - \mathbf{x}^0)$ for $t \in [0,1]$. Together with the black-box, this line induces a curve in latent space $\mathbf{g} \circ \boldsymbol{\gamma}^c : [0,1] \to \mathcal{H}$ that goes from the baseline latent representation $\mathbf{h}^0$ to the corpus example latent representation $\mathbf{h}^c$. Let us now use an infinitesimal decomposition of this curve to make the contribution of each input feature explicit. If we assume[4] that $\mathbf{g}$ is almost everywhere differentiable, we can use a first order approximation of the curve at the vicinity of $t \in (0,1)$ to decompose the infinitesimal shift in latent space:

$$\begin{aligned}\underbrace{\mathbf{g} \circ \boldsymbol{\gamma}^c(t + \delta t) - \mathbf{g} \circ \boldsymbol{\gamma}^c(t)}_{\text{Infinitesimal shift in latent space}} &= \sum_{i=1}^{d_X} \left.\frac{\partial \mathbf{g}}{\partial x_i}\right|_{\boldsymbol{\gamma}^c(t)} \left.\frac{d\gamma_i^c}{dt}\right|_t \delta t + o(\delta t) \\ &= \sum_{i=1}^{d_X} \left.\frac{\partial \mathbf{g}}{\partial x_i}\right|_{\boldsymbol{\gamma}^c(t)} (x_i^c - x_i^0) \cdot \delta t + o(\delta t),\end{aligned}$$

where we used $\gamma_i^c(t) = x_i^0 + t \cdot (x_i^c - x_i^0)$ to obtain the second equality. In this decomposition, each input feature contributes additively to the infinitesimal shift in latent space. It follows trivially that the contribution of the input feature corresponding to input dimension $i \in [d_X]$ is given by

$$\delta \mathbf{j}_i^c(t) = (x_i^c - x_i^0) \cdot \left.\frac{\partial \mathbf{g}}{\partial x_i}\right|_{\boldsymbol{\gamma}^c(t)} \delta t \qquad \in \mathcal{H}.$$

In order to compute the overall contribution of feature i to the shift, we let $\delta t \to 0$ and we integrate the infinitesimal contributions along the line $\boldsymbol{\gamma}^c$. This motivates the following definition.

[4] This is not restrictive, DNNs with ReLU activation functions satisfy this assumption for instance.

Definition 2.3 (Integrated Jacobian & Projection)**.** The *integrated Jacobian* between a baseline $(\mathbf{x}^0, \mathbf{h}^0 = \mathbf{g}(\mathbf{x}^0))$ an a corpus example $(\mathbf{x}^c, \mathbf{h}^c = \mathbf{g}(\mathbf{x}^c)) \in \mathcal{X} \times \mathcal{H}$ associated to feature $i \in [d_X]$ is

$$\mathbf{j}_i^c = \left(x_i^c - x_i^0\right) \int_0^1 \frac{\partial \mathbf{g}}{\partial x_i}\bigg|_{\boldsymbol{\gamma}^c(t)} dt \qquad \in \mathcal{H},$$

where $\boldsymbol{\gamma}^c(t) \equiv \mathbf{x}^0 + t \cdot \left(\mathbf{x}^c - \mathbf{x}^0\right)$ for $t \in [0,1]$. This vector indicates the shift in latent space induced by feature i of corpus example c when comparing the corpus example with the baseline. To summarize this contribution to the shift $\mathbf{h} - \mathbf{h}^0$ described in (2), we define the *projected Jacobian*

$$p_i^c = \text{proj}_{\mathbf{h}-\mathbf{h}^0}\left(\mathbf{j}_i^c\right) \equiv \frac{\langle\, \mathbf{h} - \mathbf{h}^0 \,,\, \mathbf{j}_i^c \,\rangle}{\langle\, \mathbf{h} - \mathbf{h}^0 \,,\, \mathbf{h} - \mathbf{h}^0 \,\rangle} \qquad \in \mathbb{R},$$

where $\langle \cdot, \cdot \rangle$ is an inner product for the latent space $\mathcal{H}$.

Remark 2.4. The integrated Jacobian can be seen as a latent-space generalization of Integrated Gradients [10]. In Section 1.2 of the supplementary material, we establish the relationship between the two quantities: $\text{IG}_i^c = \text{l}(\mathbf{j}_i^c)$.

We summarize the Jacobian quantities in Figure 3. By inspecting the figure, we notice that projected Jacobians encode the contribution of feature i from corpus example c to the overall shift in latent space: $p_i^c > 0$ implies that this feature creates a shift pointing in the same direction as the overall shift; $p_i^c < 0$ implies that this feature creates a shift pointing in the opposite direction and $p_i^c = 0$ implies that this feature creates a shift in an orthogonal direction. We use the projections to summarize the contribution of each feature in Figures 1 , 7 & 8. The colors green and red indicate respectively a positive and negative projection. In addition to these geometrical insights, Jacobian quantities come with natural properties.

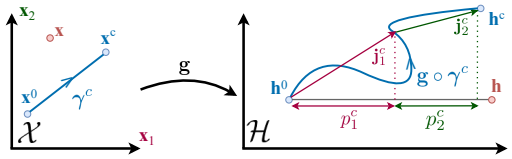

Figure 3: Integrated Jacobian and projection.

Proposition 2.1 (Properties of Integrated Jacobians)**.** *Consider a baseline* $(\boldsymbol{x}^0, \boldsymbol{h}^0 = \boldsymbol{g}(\boldsymbol{x}^0))$ *and a test example together with their latent representation* $(\boldsymbol{x}, \boldsymbol{h} = \boldsymbol{g}(\boldsymbol{x})) \in \mathcal{X} \times \mathcal{H}$*. If the shift* $\boldsymbol{h} - \boldsymbol{h}^0$ *admits a decomposition* (2)*, the following properties hold.*

$$(A): \sum_{c=1}^{C} \sum_{i=1}^{d_X} w^c \boldsymbol{j}_i^c = \boldsymbol{h} - \boldsymbol{h}^0 \qquad (B): \sum_{c=1}^{C} \sum_{i=1}^{d_X} w^c p_i^c = 1.$$

Proof. The proof is provided in Section 1.3 of the supplementary material. □

These properties show that the integrated Jacobians and their projections are the quantities that we are looking for: they transfer the corpus explanation in input space. The first equality decomposes the shift in latent space in terms of contributions $w^c \mathbf{j}_i^c$ arising from each feature of each corpus example. The second equality sets a natural scale to the contribution of each feature. For this reason, it is natural to use $w^c p_i^c$ to measure the contribution of feature i of corpus example c.

3 Experiments

In this section, we evaluate quantitatively several aspects of our method. In a first experiment, we verify that the corpus decomposition scheme described in Section 2 yields good approximations for the latent representation of test examples extracted from the same dataset as the corpus examples. In a realistic clinical use case, we illustrate the usage of SimplEx in a set-up where different corpora reflecting different datasets are used. The experiments are summarized bellow. In Section 2 of the supplementary material, we provide more details and further experiments with time series and synthetic data.

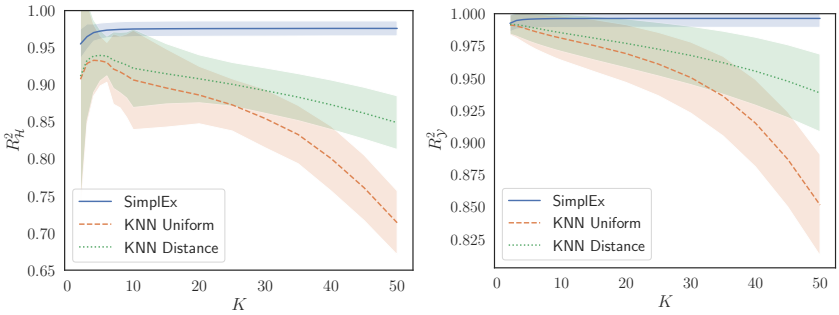

(a) R^2 score for the latent approximation (b) R^2 score for the output approximation

Figure 4: Precision of corpus decomposition for prostate cancer (avg $\pm$ std).

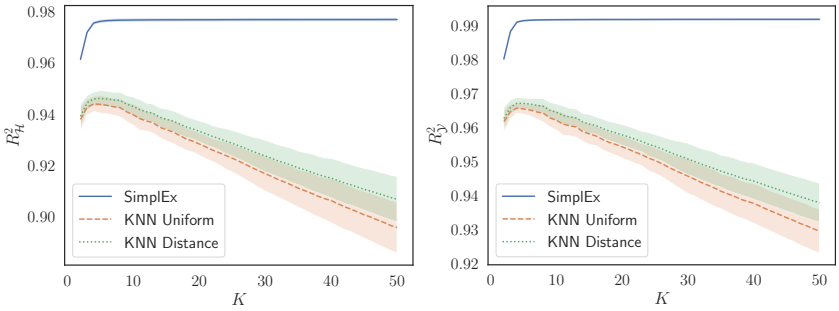

(a) R^2 score for the latent approximation (b) R^2 score for the output approximation

Figure 5: Precision of corpus decomposition for MNIST (avg $\pm$ std).

3.1 Precision of corpus decomposition

Description The purpose of this experiment is to check if the corpus decompositions described in Section 2 allows us to build good approximations of the latent representation of test examples. We start with a dataset $\mathcal{D}$ that we split into a training set $\mathcal{D}_{\text{train}}$ and a testing set $\mathcal{D}_{\text{test}}$. We train a black-box $\mathbf{f}$ for a given task on the training set $\mathcal{D}_{\text{train}}$. We randomly sample a set of corpus examples from the training set $\mathcal{C} \subset \mathcal{D}_{\text{train}}$ (we omit the true labels for the corpus examples) and a set of test examples from the testing set $\mathcal{T} \subset \mathcal{D}_{\text{test}}$. For each test example $\mathbf{x} \in \mathcal{T}$, we build an approximation $\hat{\mathbf{h}}$ for $\mathbf{h} = \mathbf{g}(\mathbf{x})$ with the corpus examples latent representations. In each case, we let the method use only K corpus examples to build the approximation. We repeat the experiment for several values of K.

Metrics We are interested in measuring the precision of the corpus approximation in latent space and in output space. To that aim, we use the R^2 score in both spaces. In this way, $R^2_{\mathcal{H}}$ measures the precision of the corpus approximation $\hat{\mathbf{h}}$ with respect to the true latent representation $\mathbf{h}$. Similarly, $R^2_{\mathcal{Y}}$ measures the precision of the corpus approximation $\hat{\mathbf{y}} = \mathbf{l}(\hat{\mathbf{h}})$ with respect to the true output $\mathbf{y} = \mathbf{l}(\mathbf{h})$. Both of these metrics satisfy $-\infty < R^2 \leq 1$. A higher R^2 score is better with $R^2 = 1$ corresponding to a perfect approximation. All the metrics are computed over the test examples $\mathcal{T}$. The experiments are repeated 10 times to report standard deviations across different runs.

Baselines We compare our method[5] (SimplEx) with 3 baselines. A first alternative, inspired by [23], is to use the K-nearest corpus neighbours *in latent space* to build the latent approximation $\hat{\mathbf{h}}$. Building on this idea, we introduce two baselines (1) KNN Uniform that takes the average latent representation of the K-nearest corpus neighbours of $\mathbf{h}$ in latent space (2) KNN Distance that computes the same average with weights w^c inversely proportional to the distance $\| \mathbf{h} - \mathbf{h}^c \|_{\mathcal{H}}$. Finally, we use the representer theorem [24] to produce an approximation $\hat{\mathbf{y}}$ of $\mathbf{y}$ with the corpus $\mathcal{C}$. Unlike the other methods, the representer theorem does not allow to produce an approximation in latent space.

[5]To enforce SimplEx to select K examples, we add a L^1 penalty making the $C - K$ smallest weights vanish.

Datasets We use two different datasets with distinct tasks for our experiment: (1) 240,486 patients enrolled in the American SEER program [26]. We consider the binary classification task of predicting cancer mortality for patients with prostate cancer. We train a multilayer perceptron (MLP) for this task. Since this task is simple, we show that a corpus of $C = 100$ patients yields good approximations. (2) 70,000 MNIST images of handwritten digits [27]. We consider the multiclass classification task of identifying the digit represented on each image. We train a convolutional neural network (CNN) for the image classification. This classification task is more complex than the previous one (higher d_X and d_Y), we show that a corpus of $C = 1,000$ images yields good approximations in this case.

Results The results for SimplEx and the KNN baselines are presented in Figure 4 & 5. Several things can be deduced from these results: (1) It is generally harder to produce a good approximation in latent space than in output space as $R^2_{\mathcal{H}} < R^2_{\mathcal{Y}}$ for most examples (2) SimplEx produces the most accurate approximations, both in latent and output space. These approximations are of high quality with $R^2 \approx 1$. (3) The trends are qualitatively different between SimplEx and the other baselines. The accuracy of SimplEx increases with K and stabilizes when a small number of corpus members contribute ($K = 5$ in both cases). The accuracy of the KNN baselines increases with K, reaches a maximum for a small K ($K = 7$ in both cases) and steadily decreases for larger K. This can be understood easily: when K increases beyond the number of relevant corpus examples, irrelevant examples will be added in the decomposition. SimplEx will typically annihilate the effect of these irrelevant examples by setting their weights w^c to zero in the corpus decomposition. The KNN baselines include the irrelevant corpus members in the decomposition, which alters the quality of the approximation. This suggests that K has to be tuned for each example with KNN baselines, while the optimal number of corpus examples to contribute is learned by SimplEx. (4) The standard deviations indicate that the performances of SimplEx are more consistent across different runs. This is particularly true in the prostate cancer experiment, where the corpus size C is smaller. This suggests that SimplEx is more robust than the baselines. (5) For the representer theorem, we have $R^2_{\mathcal{Y}} = -(6.6 \pm 6.1) \cdot 10^7$ for the prostate cancer dataset and $R^2_{\mathcal{Y}} = -(7.2 \pm 6.6)$ for MNIST. This corresponds to poor estimations of the black-box output. We propose some hypotheses to explain this observation in Section 2.1 of the supplementary material.

3.2 Use case: clinical risk model across countries

Very often, clinical risk models are produced and validated with the data of patients treated at a single site [28]. This can cause problems when these models are deployed at different sites for two reasons: (1) Patients from different sites can have different characteristics (2) Rules that are learned for one site might not be true for another site. One possible way to alleviate this problem would be to detect patients for which the model prediction is highly extrapolated and/or ambiguous. In this way, doctors from different sites can make an enlightened use of the risk model rather than blindly believing the model's predictions. We demonstrate that SimplEx provides a natural framework for this set-up.

As in the previous experiment, we consider a dataset $\mathcal{D}_{\text{USA}}$ containing patients enrolled in the American SEER program [26]. We train and validate an MLP risk model with $\mathcal{D}_{\text{USA}}$. To give a realistic realization of the above use-case, we assume that we want to deploy this risk model in a different site: the United Kingdom. For this purpose, we extract $\mathcal{D}_{\text{UK}}$ from the set of 10,086 patients enrolled in the British Prostate Cancer UK program [29]. These patients are characterized by the same features for both $\mathcal{D}_{\text{UK}}$ and $\mathcal{D}_{\text{USA}}$. However, the datasets $\mathcal{D}_{\text{UK}}$ and $\mathcal{D}_{\text{USA}}$ differ by a covariate shift: patients from $\mathcal{D}_{\text{UK}}$ are in general older, with higher Gleason scores and at earlier clinical stages.

When comparing the two populations in terms of the model, a first interesting question to ask is whether the the covariate shift between $\mathcal{D}_{\text{USA}}$ and $\mathcal{D}_{\text{UK}}$ affects the model representation. To explore this question, we take a first corpus of American patients $\mathcal{C}_{\text{USA}} \subset \mathcal{D}_{\text{USA}}$. If there is indeed a difference in terms of the latent representations, we expect the representations of test examples from $\mathcal{D}_{\text{UK}}$ to be less closely approximated by their decomposition with respect to $\mathcal{C}_{\text{USA}}$. If this is true, the corpus residuals associated to examples of $\mathcal{D}_{\text{UK}}$ will typically larger than the ones associated to $\mathcal{D}_{\text{USA}}$. To evaluate this quantitatively, we consider a mixed set of test examples $\mathcal{T}$ sampled from both $\mathcal{D}_{\text{UK}}$ and $\mathcal{D}_{\text{USA}}$: $\mathcal{T} \subset \mathcal{D}_{\text{UK}} \sqcup \mathcal{D}_{\text{USA}}$. We sample 100 examples from both sources: $|\mathcal{T} \cap \mathcal{D}_{\text{UK}}| = |\mathcal{T} \cap \mathcal{D}_{\text{USA}}| = 100$. We then approximate the latent representation of each example $\mathbf{h} \in \mathbf{g}(\mathcal{T})$ and compute the associated corpus residual $r_{\mathcal{C}}(\mathbf{h})$. We sort the test examples from $\mathcal{T}$ by decreasing order of corpus residual and we use this sorted list to see if we can detect the examples from $\mathcal{D}_{\text{UK}}$. We use previous baselines for comparison, results are shown in Figure 6.

Several things can be deduced from this experiment. (1) The results strongly suggest that the difference between the two datasets $\mathcal{D}_{\text{USA}}$ and $\mathcal{D}_{\text{UK}}$ is reflected in their latent representations. (2) The corpus residuals from SimplEx offer the most reliable way to detect examples that are different from the corpus examples $\mathcal{C}_{\text{USA}}$. None of the methods matches the ideal baseline since some examples of $\mathcal{D}_{\text{USA}}$ resemble examples from $\mathcal{D}_{\text{UK}}$. (3) When the corpus examples are representative of the training set, as it is the case in the experiment, our approach based on SimplEx provides a systematic way to detect test examples that have representations that are different from the ones produced at training time. A doctor should be more sceptical with respect to model predictions associated to larger residual with respect to $\mathcal{C}_{\text{USA}}$ as these arise from an extrapolation region of the latent space.

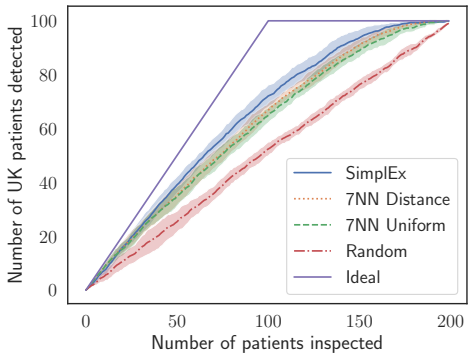

Figure 6: Detecting UK patients (avg.±std.).

Let us now make the case more concrete. Suppose that an American and a British doctor use the above risk model to predict the outcome for their patients. Each doctor wants to decompose the predictions of the model in terms of patients they knows. Hence, the American doctor selects a corpus of American patients $\mathcal{C}_{\text{USA}} \subset \mathcal{D}_{\text{USA}}$ and the British doctor selects a corpus of British patients $\mathcal{C}_{\text{UK}} \subset \mathcal{D}_{\text{UK}}$. Both corpus have the same size $C_{\text{USA}} = C_{\text{UK}} = 1,000$. We suppose that the doctors know the model prediction and the true outcome for each patient in their corpus. Both doctors are sceptical about the risk model and want to use SimplEx to decide when it can be trusted. This leads them to a natural question: is it possible to anticipate misclassification with the help of SimplEx?

In Figure 7 & 8, we provide two typical examples of misclassified British patients from $\mathcal{D}_{\text{UK}} \setminus \mathcal{C}_{\text{UK}}$ together with their decomposition in terms of the two corpora $\mathcal{C}_{\text{USA}}$ and $\mathcal{C}_{\text{UK}}$. These two examples exhibit two qualitatively different situations. In Figure 7, both the American and the British doctors make the same observation: the model relates the test patient to corpus patients that are mostly misclassified by the model. With the help of SimplEx, both doctors will rightfully be sceptical with respect to the model's prediction.

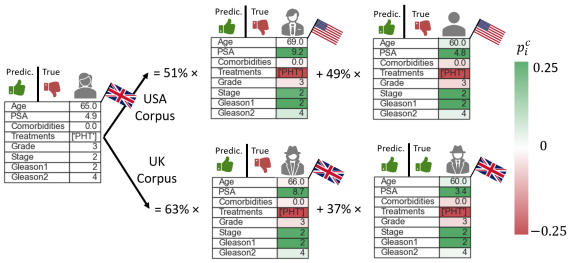

Figure 7: A first misclassified patient.

In Figure 8, something even more interesting occurs: the two corpus decompositions suggest different conclusions. In the American doctor's perspective, the prediction for this patient appears perfectly coherent as all patients in the corpus decomposition have very similar features and all of them are rightfully classified. On the other hand, the British doctor will reach the opposite conclusion as the most relevant corpus patient is misclassified by the model. In this case, we have a perfect illustration of the limitation of the transfer of a risk model from one site (America) to another (United Kingdom): similar patients from different sites can have different outcomes. In both cases, since the test patient is British, only the decomposition in terms of $\mathcal{C}_{\text{UK}}$ really matters. In both cases, the British doctor could have anticipated the misclassification of each patient with SimplEx.

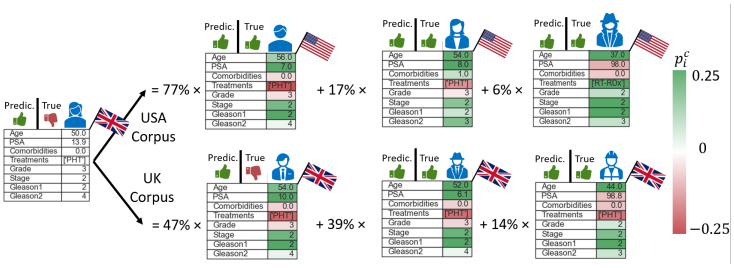

Figure 8: A second misclassified patient.

References

[1] Zachary C. Lipton. The Mythos of Model Interpretability. *Communications of the ACM*, 61(10):35–43, jun 2016.

[2] Travers Ching, Daniel S. Himmelstein, Brett K. Beaulieu-Jones, Alexandr A. Kalinin, Brian T. Do, Gregory P. Way, Enrico Ferrero, Paul-Michael Agapow, Michael Zietz, Michael M. Hoffman, Wei Xie, Gail L. Rosen, Benjamin J. Lengerich, Johnny Israeli, Jack Lanchantin, Stephen Woloszynek, Anne E. Carpenter, Avanti Shrikumar, Jinbo Xu, Evan M. Cofer, Christopher A. Lavender, Srinivas C. Turaga, Amr M. Alexandari, Zhiyong Lu, David J. Harris, Dave DeCaprio, Yanjun Qi, Anshul Kundaje, Yifan Peng, Laura K. Wiley, Marwin H. S. Segler, Simina M. Boca, S. Joshua Swamidass, Austin Huang, Anthony Gitter, and Casey S. Greene. Opportunities and obstacles for deep learning in biology and medicine. *Journal of The Royal Society Interface*, 15(141):20170387, apr 2018.

[3] Erico Tjoa and Cuntai Guan. A Survey on Explainable Artificial Intelligence (XAI): Toward Medical XAI. *IEEE Transactions on Neural Networks and Learning Systems*, pages 1–21, 2020.

[4] Alejandro Barredo Arrieta, Natalia Díaz-Rodríguez, Javier Del Ser, Adrien Bennetot, Siham Tabik, Alberto Barbado, Salvador Garcia, Sergio Gil-Lopez, Daniel Molina, Richard Benjamins, Raja Chatila, and Francisco Herrera. Explainable Artificial Intelligence (XAI): Concepts, taxonomies, opportunities and challenges toward responsible AI. *Information Fusion*, 58(December 2019):82–115, jun 2020.

[5] Arun Das and Paul Rad. Opportunities and Challenges in Explainable Artificial Intelligence (XAI): A Survey. *arXiv*, jun 2020.

[6] Lloyd Shapley. A value for n-person games. *Contributions to the Theory of Games*, 2(28):307–317, 1953.

[7] Anupam Datta, Shayak Sen, and Yair Zick. Algorithmic Transparency via Quantitative Input Influence: Theory and Experiments with Learning Systems. In *Proceedings - 2016 IEEE Symposium on Security and Privacy, SP 2016*, pages 598–617. Institute of Electrical and Electronics Engineers Inc., aug 2016.

[8] Scott Lundberg and Su-In Lee. A Unified Approach to Interpreting Model Predictions. *Advances in Neural Information Processing Systems*, 2017-Decem:4766–4775, may 2017.

[9] Marco Tulio Ribeiro, Sameer Singh, and Carlos Guestrin. "Why should i trust you?" Explaining the predictions of any classifier. In *Proceedings of the ACM SIGKDD International Conference on Knowledge Discovery and Data Mining*, volume 13-17-Augu, pages 1135–1144. Association for Computing Machinery, aug 2016.

[10] Mukund Sundararajan, Ankur Taly, and Qiqi Yan. Axiomatic Attribution for Deep Networks. *34th International Conference on Machine Learning, ICML 2017*, 7:5109–5118, mar 2017.

[11] Amit Dhurandhar, Pin-Yu Chen, Ronny Luss, Chun-Chen Tu, Paishun Ting, Karthikeyan Shanmugam, and Payel Das. Explanations based on the Missing: Towards Contrastive Explanations with Pertinent Negatives. *Advances in Neural Information Processing Systems*, 2018-December:592–603, feb 2018.

[12] R. Caruana, H. Kangarloo, J. D. Dionisio, U. Sinha, and D. Johnson. Case-based explanation of non-case-based learning methods. *AMIA Symposium*, pages 212–215, 1999.

[13] Isabelle Bichindaritz and Cindy Marling. Case-based reasoning in the health sciences: What's next? In *Artificial Intelligence in Medicine*, volume 36, pages 127–135. Elsevier, feb 2006.

[14] Mark T. Keane and Eoin M. Kenny. How Case-Based Reasoning Explains Neural Networks: A Theoretical Analysis of XAI Using Post-Hoc Explanation-by-Example from a Survey of ANN-CBR Twin-Systems. In *Lecture Notes in Computer Science (including subseries Lecture Notes in Artificial Intelligence and Lecture Notes in Bioinformatics)*, volume 11680 LNAI, pages 155–171. Springer Verlag, sep 2019.

[15] Been Kim, Cynthia Rudin, and Julie Shah. The Bayesian Case Model: A Generative Approach for Case-Based Reasoning and Prototype Classification. *Advances in Neural Information Processing Systems*, 3(January):1952–1960, mar 2015.

[16] Been Kim, Rajiv Khanna, and Oluwasanmi Koyejo. Examples are not Enough, Learn to Criticize! Criticism for Interpretability. Technical report, 2016.

[17] Karthik S. Gurumoorthy, Amit Dhurandhar, Guillermo Cecchi, and Charu Aggarwal. Efficient Data Representation by Selecting Prototypes with Importance Weights. *Proceedings - IEEE International Conference on Data Mining, ICDM*, pages 260–269, jul 2017.

[18] R. Dennis Cook and Sanford Weisenberg. *Residuals and influence in regression*. New york: Chapman and hall edition, 1982.

[19] Pang Wei Koh and Percy Liang. Understanding Black-box Predictions via Influence Functions. *34th International Conference on Machine Learning, ICML 2017*, 4:2976–2987, mar 2017.

[20] Amirata Ghorbani and James Zou. Data Shapley: Equitable Valuation of Data for Machine Learning. *36th International Conference on Machine Learning, ICML 2019*, 2019-June:4053–4065, apr 2019.

[21] Amirata Ghorbani, Michael P. Kim, and James Zou. A Distributional Framework for Data Valuation. *arXiv*, feb 2020.

[22] Been Kim, Martin Wattenberg, Justin Gilmer, Carrie Cai, James Wexler, Fernanda Viegas, and Rory Sayres. Interpretability Beyond Feature Attribution: Quantitative Testing with Concept Activation Vectors (TCAV). *35th International Conference on Machine Learning, ICML 2018*, 6:4186–4195, nov 2017.

[23] Nicolas Papernot and Patrick McDaniel. Deep k-Nearest Neighbors: Towards Confident, Interpretable and Robust Deep Learning. *arXiv*, mar 2018.

[24] Chih-Kuan Yeh, Joon Sik Kim, Ian E. H. Yen, and Pradeep Ravikumar. Representer Point Selection for Explaining Deep Neural Networks. *Advances in Neural Information Processing Systems*, 2018-December:9291–9301, nov 2018.

[25] Mark T. Keane and Eoin M. Kenny. The Twin-System Approach as One Generic Solution for XAI: An Overview of ANN-CBR Twins for Explaining Deep Learning. *arXiv*, may 2019.

[26] Surveillance Research Program National Cancer Institute, DCCPS. Surveillance, epidemiology, and end results (seer) program. www.seer.cancer.gov.

[27] Li Deng. The mnist database of handwritten digit images for machine learning research. *IEEE Signal Processing Magazine*, 29(6):141–142, 2012.

[28] Eric Wu, Kevin Wu, Roxana Daneshjou, David Ouyang, Daniel E Ho, and James Zou. How medical AI devices are evaluated: limitations and recommendations from an analysis of FDA approvals. *Nature Medicine*, 2021.

[29] Prostate Cancer UK. Cutract. www.prostatecanceruk.org.

[30] Rushil Anirudh, Jayaraman J. Thiagarajan, Rahul Sridhar, and Peer-Timo Bremer. MARGIN: Uncovering Deep Neural Networks using Graph Signal Analysis. *arXiv*, nov 2017.

[31] Gregory Cohen, Saeed Afshar, Jonathan Tapson, and André van Schaik. EMNIST: an extension of MNIST to handwritten letters. feb 2017.

[32] Alberto Abadie. Using Synthetic Controls: Feasibility, Data Requirements, and Methodological Aspects. *Journal of Economic Literature*, 2020.

[33] Alberto Abadie, Alexis Diamond, Hainmueller, and Jens. Synthetic control methods for comparative case studies: Estimating the effect of California's Tobacco control program. *Journal of the American Statistical Association*, 105(490):493–505, jun 2010.

[34] Susan Athey, Mohsen Bayati, Nikolay Doudchenko, Guido Imbens, and Khashayar Khosravi. Matrix Completion Methods for Causal Panel Data Models. *arXiv*, oct 2017.

[35] Muhammad Amjad, Devavrat Shah, and Dennis Shen. Robust Synthetic Control. Technical Report 22, 2018.

[36] Ruth C. Fong and Andrea Vedaldi. Interpretable Explanations of Black Boxes by Meaningful Perturbation. *Proceedings of the IEEE International Conference on Computer Vision*, 2017-Octob:3449–3457, 2017.

[37] Ruth Fong, Mandela Patrick, and Andrea Vedaldi. Understanding deep networks via extremal perturbations and smooth masks. *Proceedings of the IEEE International Conference on Computer Vision*, 2019-Octob:2950–2958, 2019.

Checklist

1. For all authors...
   (a) Do the main claims made in the abstract and introduction accurately reflect the paper's contributions and scope? [Yes] All the claims made about SimplEx are verified in Section 3 and Section 2 of the supplementary material.
   (b) Did you describe the limitations of your work? [Yes] Assumption 2.1 describes the class of model for which our work applies.
   (c) Did you discuss any potential negative societal impacts of your work? [Yes] SimplEx only allows to make machine learning models more easily interpretable to a human audience. We don't see any negative societal impact of providing more transparency in machine learning. We have carefully checked the list of potential negative societal impacts provided on NeurIPS website and found that none of them applies to our method.
   (d) Have you read the ethics review guidelines and ensured that your paper conforms to them? [Yes] We have carefully read the ethics review guideline and we can confirm that our paper respects the guidelines.
2. If you are including theoretical results...
   (a) Did you state the full set of assumptions of all theoretical results? [Yes] All the assumptions required for the theorem to hold are stated rigorously in Section 2.
   (b) Did you include complete proofs of all theoretical results? [Yes] Proofs for the theoretical results are provided in Section 1 of the supplementary material.
3. If you ran experiments...
   (a) Did you include the code, data, and instructions needed to reproduce the main experimental results (either in the supplemental material or as a URL)? [No] The code for our method will be made public at publication.
   (b) Did you specify all the training details (e.g., data splits, hyperparameters, how they were chosen)? [Yes] All the details about the experiments are provided in Section 3 and Section 2 of the supplementary material.
   (c) Did you report error bars (e.g., with respect to the random seed after running experiments multiple times)? [Yes] See Figure 4, 5 & 6.
   (d) Did you include the total amount of compute and the type of resources used (e.g., type of GPUs, internal cluster, or cloud provider)? [Yes] See Section 2 of the supplementary material
4. If you are using existing assets (e.g., code, data, models) or curating/releasing new assets...
   (a) If your work uses existing assets, did you cite the creators? [Yes] See references [27, 31, 26, 29], all of them are cited in the paper or the supplementary material.
   (b) Did you mention the license of the assets? [Yes] The license are mentioned in Section 2 of the supplementary material.
   (c) Did you include any new assets either in the supplemental material or as a URL? [N/A]

(d) Did you discuss whether and how consent was obtained from people whose data you're using/curating? [N/A]

(e) Did you discuss whether the data you are using/curating contains personally identifiable information or offensive content? [N/A]

5. If you used crowdsourcing or conducted research with human subjects...

(a) Did you include the full text of instructions given to participants and screenshots, if applicable? [N/A]

(b) Did you describe any potential participant risks, with links to Institutional Review Board (IRB) approvals, if applicable? [N/A]

(c) Did you include the estimated hourly wage paid to participants and the total amount spent on participant compensation? [N/A]